Dynamic and Control of a Heterogeneous Azeotropic Distillation Column: Conventional Control Approach

ARTICLE *in* INDUSTRIAL & ENGINEERING CHEMISTRY RESEARCH · FEBRUARY 1999

Impact Factor: 2.59 · DOI: 10.1021/ie980269f

Dynamics and Control of a Heterogeneous Azeotropic Distillation Column: Conventional Control Approach

I-L. Chien*

Department of Chemical Engineering, National Taiwan University of Science and Technology, Taipei, Taiwan 10672

C. J. Wang and D. S. H. Wong

Department of Chemical Engineering, National Tsing Hua University, Hsinchu, Taiwan 30043

In this work, bifurcation analysis and dynamic simulation were used to investigate the optimum conventional control strategy of an isopropyl alcohol (IPA), cyclohexane (CyH), and water (H_2O) heterogeneous azeotropic column. Steady-state process analysis shows that the optimal operation point should be located at a critical reflux, a transition point at which the distillation path switches from a route that passes through the IPA + H_2O azeotrope to one that passes through the IPA + CyH azeotrope. A good control strategy must be able to maintain a steady column temperature profile that shows a plateau near 70 °C to ensure passage around the IPA + CyH azeotrope. An inverse double-loop control strategy is proposed based on principal component analysis. This scheme is capable of maintaining the desired column temperature profile given all kinds of feed disturbances, thus keeping the product IPA purity at the desired level.

1. Introduction

Heterogeneous azeotropic distillation is a special distillation process developed to break azeotrope or separate close boiling mixtures. However, the steady-state and dynamic behavior of the process is complex and quite difficult to control. A recent review by Widagdo and Seider[1] showed that parametric sensitivity, multiple steady states, long transient, and nonlinear dynamics were found by many authors using theoretical models and computer simulation and, recently, with experimental verification (Prokopakis and Seider,[2,3] Kovach and Seider,[4,5] Pham et al.,[6] Ryan and Doherty,[7] Widagdo et al.,[8] Cairns and Furzer,[9−11] Pham and Doherty,[12−14] Rovaglio and Doherty,[15] Wong et al.,[16] Widagdo et al.,[17] Furzer,[18] Gani and Jørgensen,[19] Bekiaris et al.,[20] Müller et al.,[21] Müller and Marquardt,[22] and Wang et al.[23]). However, most of the literatures on this topic are concerned mainly with process design and system characteristics. There have been relatively little discussions about control of heterogeneous azeotropic distillation. Bozenhardt[24] proposed control strategy involving average temperature control, on-line break point position control, and five feedforward control loops for the ethanol + ether + water system. On-line tests by the author claimed to reduce energy consumption compared to the traditional control scheme, but no detailed performance data were available. Rovaglio et al.[25] proposed average temperature control and two feedforward control loops for the ethanol + benzene + water system. One of the feedforward loops controls the inventory of the entrainer, while the other modifies the set point of the average temperature loop. Both of the strategies proposed by Bozenhardt[24] and Rovaglio et al.[25] require either on-line composition measurement or a precise mathematical model of the system to proceed with the feedforward controls. They would be expensive to implement in a real plant.In this work, bifurcation analysis, dynamic simulation, and principal component analysis were used to investigate the possibility of using conventional temperature control strategy to effectively control an isopropyl alcohol (IPA), cyclohexane (CyH), and water (H_2O) heterogeneous azeotropic column.

* Corresponding author. Phone: +886-2-2737-6652. Fax: +886-2-2737-6644. E-mail: Chien@ch.ntust.edu.tw.

2. Process Characteristics

Process Model Description. In our preceding paper, Wang et al.[23] used bifurcation analysis with a software package (AUTO) developed by Doedel and Wang[26] and a dynamic simulation algorithm to examine a heterogeneous distillation column. This simulated column has 28 equilibrium stages, including condenser−decanter (stage 1) and reboiler (stage 28) with the feed stream at stage 4. The feed flow rate is 1 mol/min, containing 69 mol % IPA and 31 mol % H_2O. The entrainer makeup flow rate is 0.03 mol/min and adds to the decanter. The overall process flow diagram is shown in Figure 1. The overhead vapor from the column is subcooled in the condenser with a constant temperature of 298 K into the decanter. The feed temperature is 298 K. The column is operating at atmospheric pressure, with the pressure drop inside the column assumed negligible. The overall column tray efficiency is assumed to be ideal. The residual curve map of this IPA + CyH + H_2O system can be seen in Wang et al.[23]

For bifurcation analysis, constant molar overflow is assumed to reduce the dimensionality of the system equation. Heterogeneous liquid-phase split was allowed in any stage. Following Schuil and Bool,[27] the steady-state balance equations were expressed as the "overall" liquid composition, and K values were defined as the average properties of the two coexisting liquid phases. The tangent plane analysis (Michelsen[28]) was used to check for possible phase splitting for the "overall" liquid composition. Bubble-point or vapor−liquid−liquid equilibrium (VLLE) calculations were used to calculate the

10.1021/ie980269f CCC: $18.00
Published on Web 01/12/1999

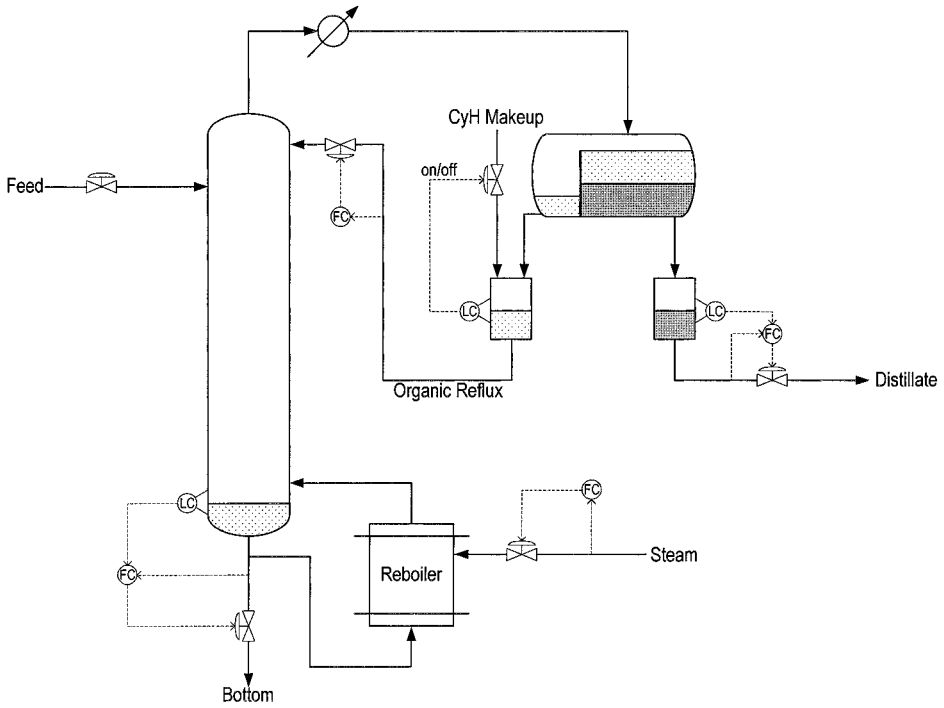

Figure 1. Simplified process flow diagram of the column system.

K values accordingly with the coefficients for the thermodynamic models [Antoine and nonrandom two liquid (NRTL)] taken from work by Wang et al.[23] The qualitative features of the steady-state behavior are consistent with those obtained using dynamic simulation and confirmed by experiment in work by Wang et al..[23]

Dynamic Simulation. The dynamic simulation model is a rigorous transient material and energy balance equilibrium stage model. The column specifications were the same as those for bifurcation analysis, except that the constant molar overflow assumption was removed. In addition to the "overall" liquid composition and the "average" *K* values, average liquid flows and holdup were also used in the dynamic simulation. The material balance equations were integrated by a third-order semi-implicit Runge−Kutta method to obtain overall liquid flow rates and liquid compositions. The tangent plane analysis (Michelsen[28]) was also used in the dynamic simulation to check for possible phase splitting for a given average composition. Bubble-point or VLLE calculations were used to update the average *K* values. Liquid holdups were calculated by Frances' weir equation and overall liquid flow. Vapor flows were obtained by enthalpy balance. Details of the simulation algorithm were furnished by Wong et al.[16]

A feed flow rate of 1 mol/min was used in all of our simulations. The volume of reboiler and decanter holdups were both 500 mL. The weir constants were set so that the ratio of the tray holdup to the feed rate was approximately 0.055 min. In the dynamic simulation, the decanter aqueous-phase level was perfectly controlled by the aqueous distillate draw rate. The decanter organic-phase level was maintained by an on−off control using entrainer makeup. Although a water bleed line in the condenser or decanter is commonly used in the industry of anhydrous alcohol production to enhance the chance that the top tray will produce a mixture with bulk composition inside the immiscible region, it is not considered in this simulation.

Bifurcation Analysis. Figure 2 shows the relationship between the bottom composition (IPA) and the vapor boilup rate, with reflux being fixed at 1.0 mol/min obtained using bifurcation analysis. There are three branches of steady state. The upper and lower branches are stable, while the middle branch is unstable. There exist three steady states when the vapor flow rate ranges from about 1.2 to 1.6 mol/min at this reflux. The vapor rate achieving the highest attainable purity is at about 1.591 mol/min. Around this vapor rate, three very different steady-state column profiles can be found. Type I can be found along the top branch. Type II can be found at a small portion of the upper branch near the turning point at 1.591 mol/min. Type III is associated with the bottom branch and the unstable branch. Three plateaus, one at the top of the column at 64.3 °C, one at 69.3 °C which is the boiling point of the IPA + CyH azeotrope, and one at the bottom of the column at 82.5 °C, characterize a type II profile. For this type of operation, there is excess cyclohexane in the column to ensure that all of the water in the feed is entrained out as the ternary azeotrope. The first temperature rising front from the plateau at 64.3 °C to one at 69.3 °C represents the separation of the ternary azeotrope and the binary azeotrope IPA + CyH. The second rising front from the plateau at 69.3 °C to one at 82.5 °C represents the stripping of cyclohexane out of the binary azeotrope IPA + CyH. The plateau near the bottom of the column vanishes for a type I profile. This happens when the reflux is too high and there is not enough reboiled vapor to strip CyH out of IPA + CyH. In a type III profile, the plateau at 69.3 °C is lost entirely so that there is not enough CyH in the column to remove water. The distillation path passes around the IPA + H_2O azeotrope. This happens when there is not enough reflux but too much reboiled vapor so that CyH is stripped out of the column.

A type II profile represents the desired operation because high IPA purity is achieved. However, because such a steady-state profile can only be found right at

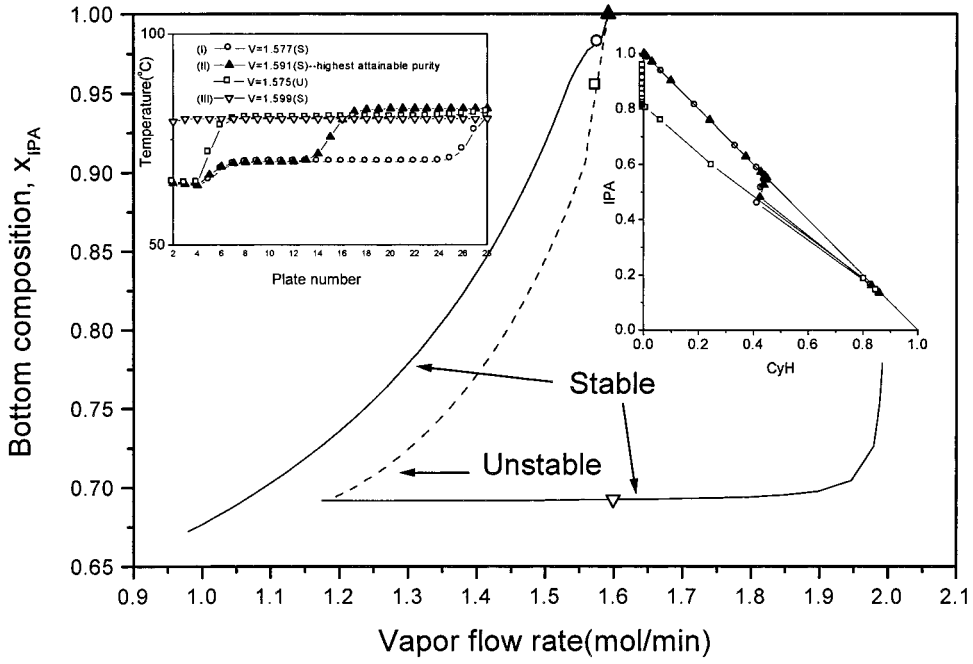

Figure 2. Bifurcation diagram for the system at an organic reflux flow of 1.0 mol/min.

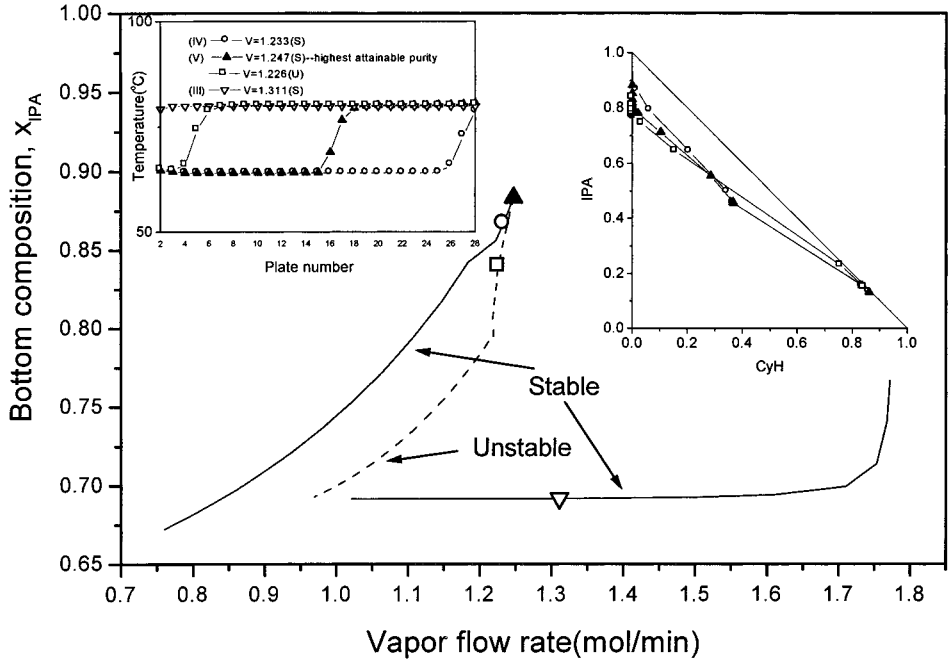

Figure 3. Bifurcation diagram for the system at an organic reflux flow of 0.78 mol/min.

the edge of the top stable branch and the middle unstable branch, it is therefore an unstable operation point. Any slight increase of the vapor boilup rate from 1.591 mol/min will cause a drastic change in the purity of the IPA product. Dorn et al.[29] discussed a similar unstable operating point in a homogeneous distillation column. In their case, however, the operating point in the middle unstable branch does not result in a high-purity product.

A similar phenomenon is observed when the reflux is reduced to a lower value of 0.78 mol/min. Figure 3 shows three branches of steady states, two stable and one unstable, in a small vapor flow rate region (1.0−1.25 mol/min). Three very different column profiles are found. A type IV profile is found along the top branch. Type V profiles can be found near the edge of the top branch. The profiles along the lower portion of the unstable branch and the bottom branch (type VI) are similar to those of type III obtained at higher reflux. A type V profile has only one temperature rising front and two plateaus (64.3 °C near the top and 82.5 °C near the bottom). There is no plateau at 69.3 °C. A lot of stages at the top have heterogeneous liquid splitting. In this kind of operation, there is not enough entrainer inside the column to remove all of the water. The distillation path passes around the IPA + H_2O azeotrope. The lower section of the column represents stripping water out of the IPA + H_2O azeotrope. If the vapor boilup rate is reduced, the temperature front moves toward the bottom of the column, resulting in a type IV profile. If the vapor boilup rate is increased, the remaining CyH is stripped out of the column. The profile changes to one

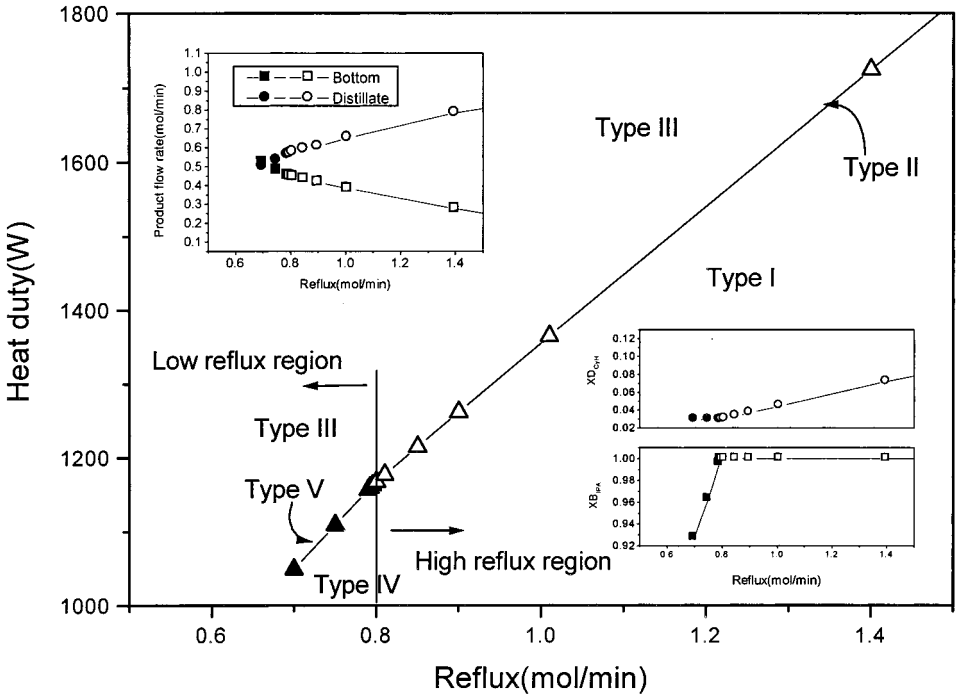

Figure 4. Process optimum operating line on the reflux-duty plane.

very similar to that of type III obtained at higher reflux. Experimental verification of the above type I−V temperature profiles in high-reflux and low-reflux regions can be seen in Wang et al.[23]

Optimum Operating Point. Bifurcation analysis shows that at each reflux there is a corresponding vapor boilup rate that achieves the highest attainable IPA purity. These turning points between the upper stable branch and the unstable branch at various refluxes and reboiler duty are located using a full dynamic equilibrium stage model run to steady states. Figure 4 shows that there is a feasible operating line on the reflux-duty plane with the feed rate fixed at 1 mol/min. In the higher reflux region, the steady state on this feasible operating line exhibits a type II profile inside the column. The column profile will transform from type II to a very different type I (or type III) when heat duty slightly decreases (or increases), accompanied by the drastic loss of IPA purity. In the lower reflux region, the feasible operating line represents a type V profile inside the column. The profile will also change from type V to a very different type IV (III) when heat duty slightly decreases (or increases), causing a significant drop of bottom product purity.

Along the feasible operating line, there is a critical reflux around 0.8 that separates the lower and higher reflux regions. At refluxes higher than this value, a type II profile with a 69.3 °C plateau is found on the feasible operation line. At refluxes lower than this value, a type V profile without a 69.3 °C plateau is found on the feasible operation line. The bottom IPA purity XB_{IPA} will drop rapidly with reflux when the operation point is situated on the feasible operating line but in the lower reflux region. It would change little when the operation point is situated on the feasible operating line but in the higher reflux region. However, on the feasible operating line but in a *much higher* reflux region, the flow rate of the bottom product will decrease substantially while that of distillate and entrainer loss will increase.

Apparently, any desirable operation that gives a high-purity IPA product must be on the feasible operating line and in the high-reflux region. However, to minimize energy consumption and maximize product recovery through the bottom product stream, the operation point must be as close to critical reflux as possible. An effective control strategy must be employed to prevent the column profile from changing from type II to others (types I, III, IV, and V).

In practical situations, locating this optimum operating point is achieved by starting up the column normally with conservatively high reflux and heat duty to ensure that a type II temperature profile can be obtained and then decreasing reflux and heat duty slowly until the 69.3 °C plateau disappeared. At this point, the reflux can be increased slightly to ensure going back to the high-reflux region in Figure 4. Because of the high sensitivity of this column system, the optimum operating point usually cannot be exactly located in practical situations. Nonetheless, with the above start-up strategy and appropriate control strategy developed in the next section to ensure a type II column temperature profile, a high-purity product and low-energy consumption can be obtained near and slightly greater than this optimal operating reflux.

3. Control Strategy Development

In the following, several different control strategies will be tested using dynamic simulation to see whether the desired column profile (type II) can be maintained under various feed disturbances. The control will be difficult because any point on the feasible operating line is an intersection between a stable and an unstable branch (cf. Dorn et al.[29]). The optimal point on this line is near the critical reflux where the temperature profile can shift from type II to type V. Open-loop responses to ±5% changes in the feed flow rate and feed composition initiated at the 50th min are shown in Figure 5. After 10 min, a +5% change in the feed flow rate will cause

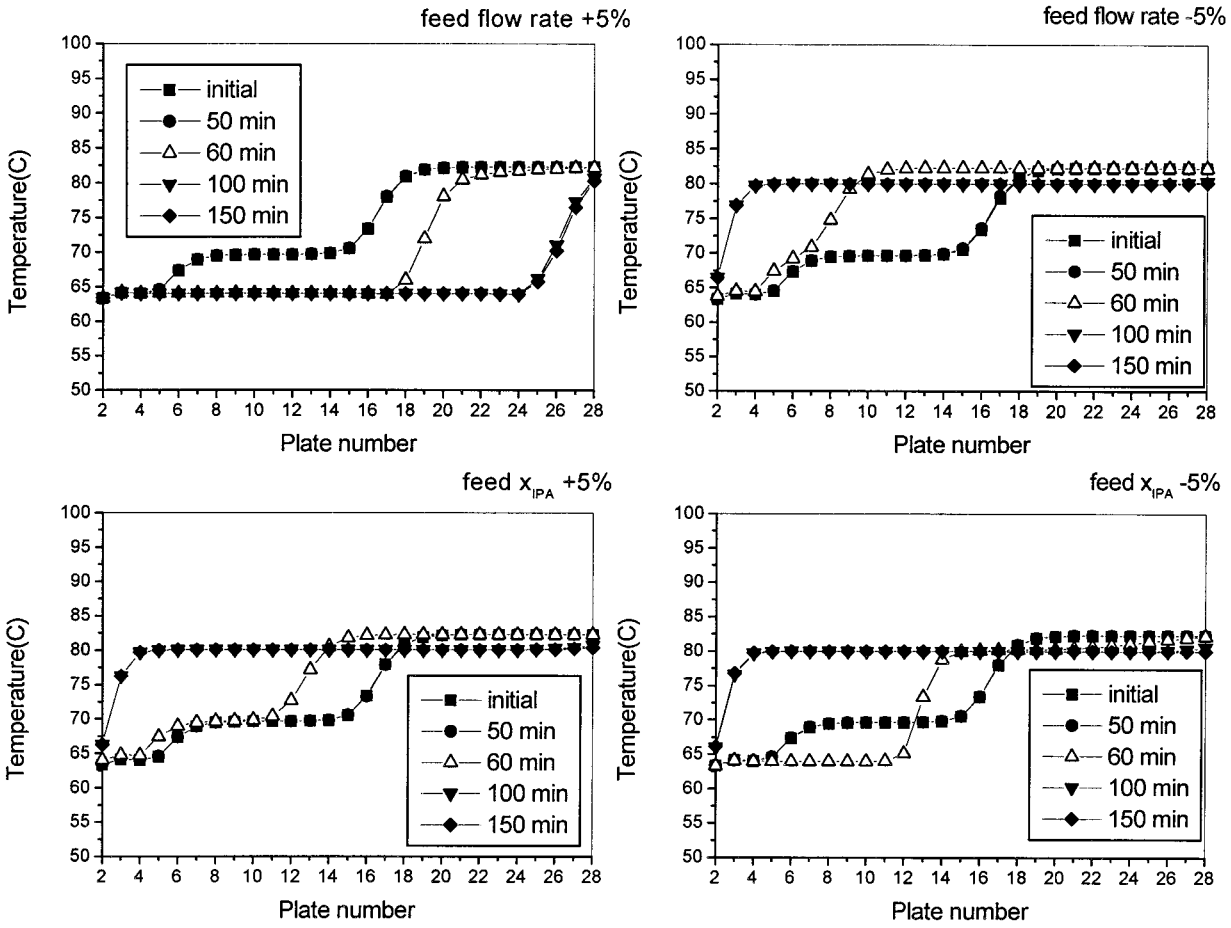

Figure 5. Open-loop tray temperature profile for the feed disturbances.

the profile to shift from a type II profile first to a type V profile and then gradually to a type IV profile in another 40 min. The bottom purity of IPA is lost completely when a type IV profile is obtained. A −5% change in the feed flow rate will make the profile shift gradually to the top of the column until the first plateau is lost. The profile will shift from a type II profile directly to a type III profile in about 50 min. A +5% change in the IPA mole fraction of the feed will have an effect similar to that of a −5% change in the feed flow rate. However, a −5% change in the IPA mole fraction of the feed will cause the profile to shift from a type II profile first to a type V profile in 10 min and then gradually to a type III profile in another 40 min. Trays 6−11 will experience inverse responses. Without control, the bottom purity of IPA is all lost to an unacceptable level.

The following assumptions in formulating the control strategy were made so that the research results can be easily applicable to industrial operation with a similar process setup:

(1) The controllers in the control strategies below are all of the PI type; no advance control method is considered.

(2) There is no on-line composition measurement; the product quality control is achieved through tray temperature control loops.

In comparison of the performance of various control strategies, the same PI tuning rule as that proposed by Chien et al.[30] is used so that any tuning effects can be ruled out. This tuning method emphasizes in the open-loop step "initial response". It is explained briefly using Figure 6, which is the open-loop response of a controlled

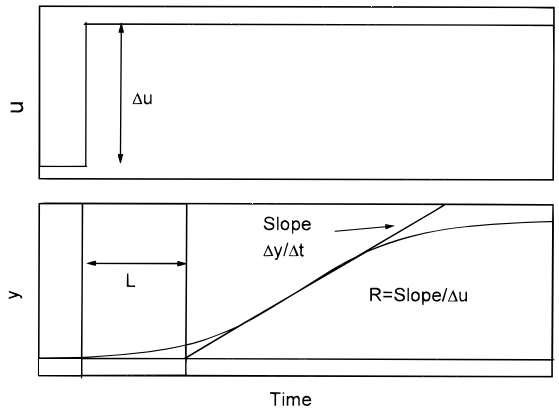

Figure 6. Open-loop step response data to obtain R and L parameters.

variable with respect to a step change in the manipulated variable. The simple loop tuning rule is

$$K_c = \frac{1}{2RL} \qquad \tau_I = 5L \tag{1}$$

where K_c is controller gain and τ_I is the reset time. With double temperature loops [for systems with relative gain array (RGA) greater than 1], to consider the interaction between the two loops, the controller parameter is detuned to be

$$K_c = \frac{7}{16RL} \qquad \tau_I = 7L \tag{2}$$

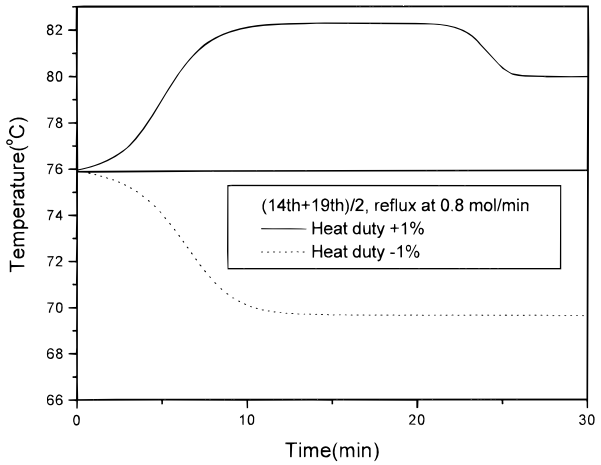

Figure 7. Open-loop step test for heat duty ±1% changes.

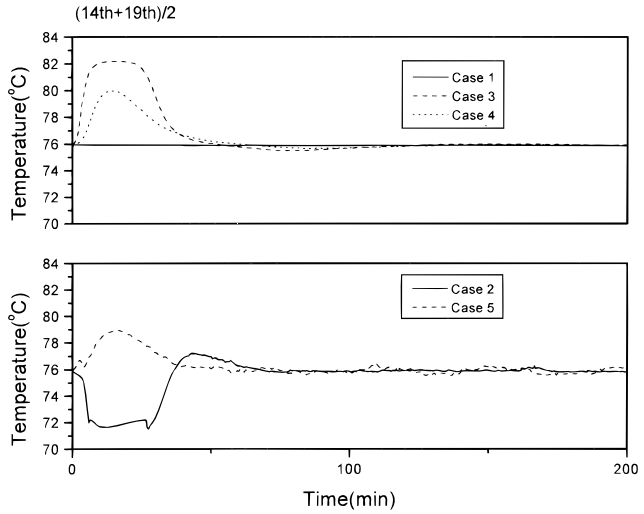

Figure 8. Closed-loop temperature dynamic response for single-loop control with two-tray temperature averaging.

The open-loop initial response parameters (R and L), which are the high-frequency information of the system, are much less susceptible to the system nonlinearities. It was shown that a better linear model for controller tuning purposes can be obtained by concentrating on fitting the initial portion of the step response (Chien and Fruehauf[31]). This philosophy has been successfully demonstrated with a highly nonlinear high-purity column example in Chien and Ogunnaike.[32]

Five feed disturbances will be considered in all of the following closed-loop tests to evaluate the disturbance rejection capability of various control strategies. They are as follows:

Case 1: feed flow rate with Gaussian noise only.

Case 2: feed flow rate (with Gaussian noise) increase of 5%.

Case 3: feed flow rate (with Gaussian noise) decrease of 5%.

Case 4: feed flow rate (with Gaussian noise) fixed, IPA content increase of 5%.

Case 5: feed flow rate (with Gaussian noise) fixed, IPA content decrease of 5%.

Single-Loop Average Temperature Control. A commonly adopted strategy is to control the average temperature of the major temperature rising front. This was employed in the schemes of Bozenhardt[24] and Rovaglio et al.[25] Here the single-loop average temperature control without any supplementary feedforward control or break point position control is evaluated. Reboiler heat duty is used to control the average temperature of the 14th and 19th tray on the major temperature front from 69.3 to 82.5 °C. The organic reflux is fixed, and the makeup flow rate is used to control the decanter organic-phase level with an on−off control mechanism. The reason to use makeup flow rate instead of organic reflux to control the decanter organic-phase level is to eliminate the disturbances of recycling effects between the column and the decanter. Other control arrangements include using the aqueous distillate draw and the bottom product draw to control the aqueous-phase level and the column bottom level, respectively.

Figure 7 is the open-loop test result. When heat duty increases by 1%, the temperature response first increases and then decreases to a constant value. The strange overshoot response is due to the fact that the

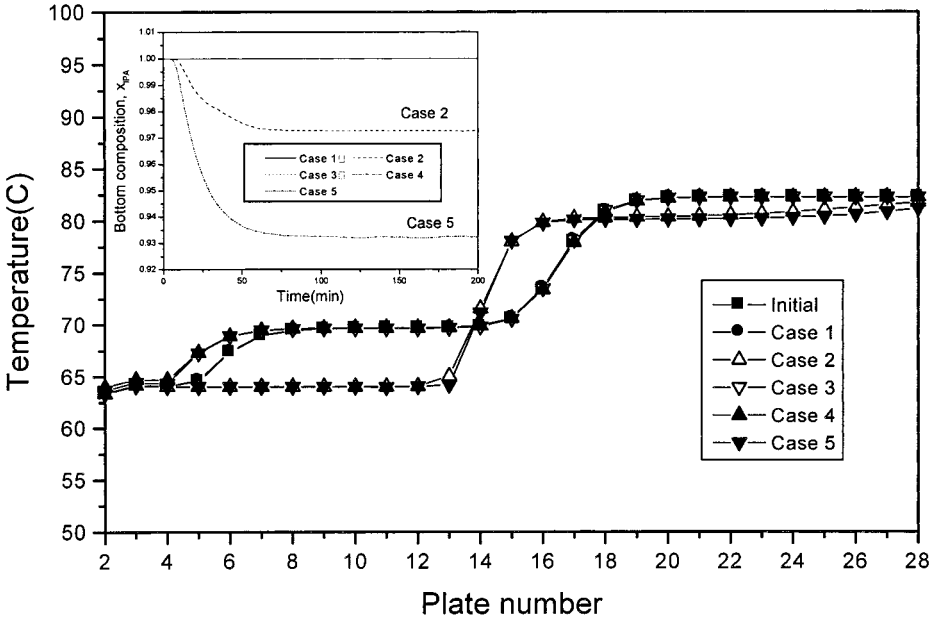

Figure 9. Closed-loop tray temperature profile and composition response for single-loop control with two-tray temperature averaging.

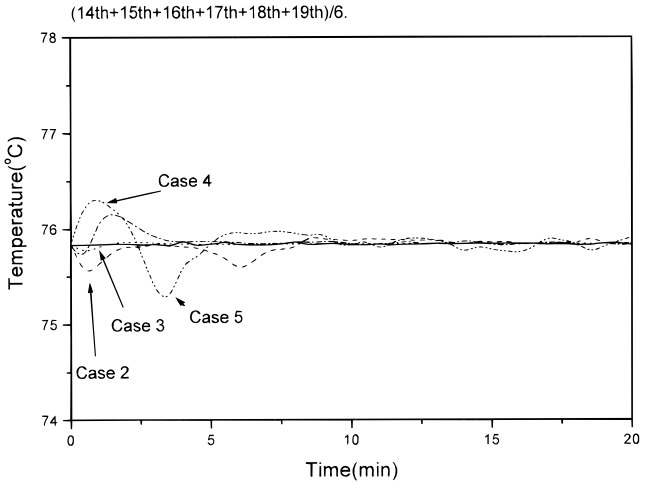

Figure 10. Closed-loop temperature dynamic response for single-loop control with major front temperature averaging.

type II profile moves up the tower initially and finally transforms into a type III profile. The entrainer inventory excluding the decanter will almost be stripped out of the column, leaving only IPA and water existing inside, and the separation fails. When heat duty decreases by 1%, the temperature response decreases and maintains at 69.3 °C (from type II to type I).

Though the open-loop response is unusual, the initial response for the first 10 min still can be used to tune a PI controller. The controlled variable response and the final temperature profiles of close-loop test results are shown in Figures 8 and 9, respectively. Figure 8 shows that the control scheme is able to hold the *controlled variable* at setpoint for all five feed disturbance cases. The closed-loop response of the controlled variable settles within 50 min. However, in cases 2 and 5, the profiles have transformed from type II to type V, accompanied by the loss of IPA purity (see Figure 9). For cases 2 and 5, the feed flow rate of water increases. The amount of entrainer inside the column required to remove all of the water increases. If we generate an operating line as shown in Figure 4 for these new feed conditions, the value of critical reflux should be higher. The new feed conditions render the system below the critical reflux in cases 2 and 5. Conversely, in cases 3 and 4, the feed flow rate of water decreases. The amount of entrainer required to remove all of the water decreases; hence, the value of critical reflux should be lower. The system remains in the high-reflux region under these two new feed conditions; the control strategy is able to preserve the desired temperature profile.

Figure 10 showed the controlled variable responses if the average temperature of all of the stages on the temperature rising front between the 14th and 19th stages is used. It was found that the average of the temperatures of all of the stages on the temperature rising front is less sensitive. Hence, tighter control action is allowed to obtain quicker closed-loop temperature response. The settling time of the closed-loop response of the controlled variable is less than 10 min. However, for cases 2 and 5, the profiles have still transformed from type II to type V, accompanied by the loss of IPA purity.

To ensure that the operation point is located on the right side of critical reflux, the reflux should increase simultaneously with an increase of the heat duty as the feed flow of water increases. This calls for ratio control strategy. We assume that the ratio of change on reflux will be the same as that on heat duty. Figure 11 shows that, using this ratio control strategy, all of disturbances except case 5 can be rejected. A different ratio is required to reject the feed composition disturbance of case 5. This is the reason why feedforward control has been suggested to supplement single-loop temperature control. The correct disturbance must be identified before the proper supplementary corrective action can be determined.

Conventional Double-Loop Temperature Control. In this section, the originally spare manipulated variable, organic reflux, is also used to control the tray temperature. An intuitive trivial thinking is to fix two temperatures near the upper and lower ends of the major temperature front. Figure 12 is the open-loop response. The nonlinear behavior of the response and interaction between loops are apparent. We use heat duty to control the temperature of the 18th plate, and

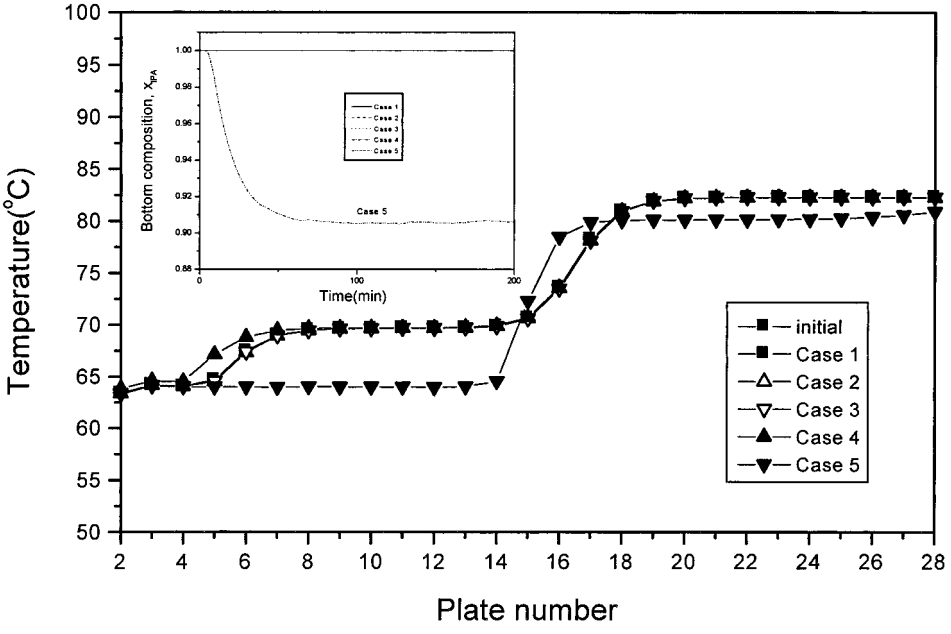

Figure 11. Closed-loop tray temperature profile and composition response for single-loop control plus ratio scheme.

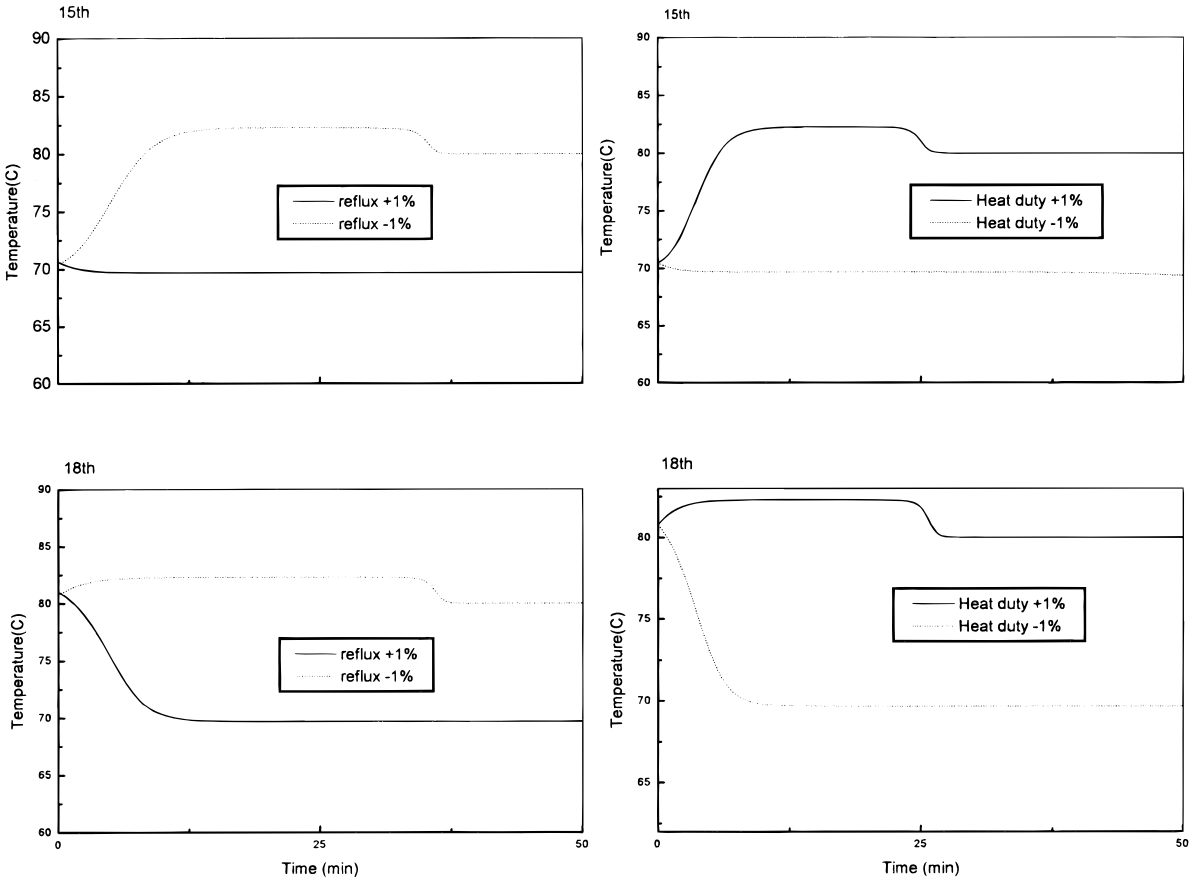

Figure 12. Open-loop step response for the 15th and 18th tray temperatures.

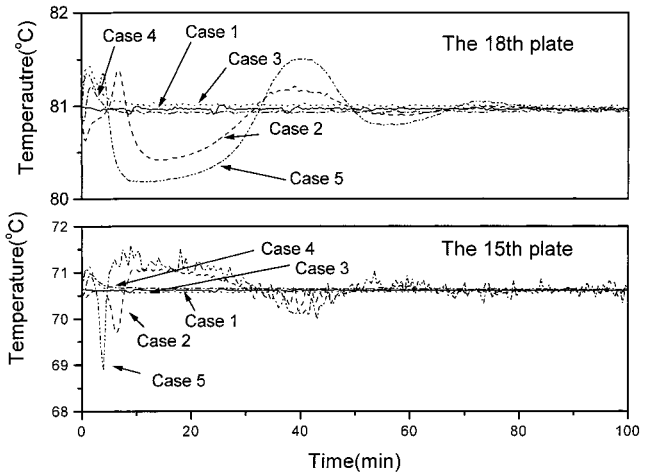

Figure 13. Closed-loop temperature dynamic response for conventional double-loop temperature control scheme.

the organic reflux is used to control the temperature of the 15th plate. The tuning constants of each control loop are averaged to get the more conservative values. Figures 13 and 14 are the close-loop responses of the controlled variables and the changes in column temperature profiles. The controller performance is worse than that of the single-loop temperature control because of strong interaction. Even though the *controlled variables* could be brought back to setpoint, the profiles still change from type II to type V for cases 2 and 5, accompanied by a small loss of bottom purity.

Inverse Double-Loop Average Temperature Control. It should also be pointed out in the above discussions, when the control scheme fails to maintain a type II profile for cases 2 and 5 disturbances, that there is no offset in the *controlled variable*. The temperature control objectives are achieved for single-loop and conventional double-loop control, but the objective of maintaining a type II profile is not achieved, resulting in loss of IPA purity. Remember that the main feature of a type II profile is the 69.3 °C plateau. To ensure that this plateau is established, there must be two temperature fronts inside the column. A major one from the boiling point of pure IPA at 82.5 °C to the boiling point of the IPA + CyH azeotrope at 69.3 °C should be found near the bottom of the column. A minor one from 69.3 °C to the boiling point of a ternary azeotrope at 64.3 °C should be found near the top section of the column. The control strategies that have been discussed so far could not guarantee the existence of the minor front. On the basis of this intuitive observation, two controlled variables are defined as the average temperature of the 4th to 8th and the 14th to 19th plates.

As an independent verification of the temperature control points, the principal component analysis described by Moore[33] is used here with a modification. In the original principal component analysis, a steady-state gain matrix is used to do singular-value decomposition as follows

$$\mathbf{K} = \mathbf{U\Sigma V}^{\mathrm{T}} \tag{3}$$

with two manipulated variables and $n = 27$ possible temperature control points. $\mathbf{K}$ is a 27×2 steady-state gain matrix. $\mathbf{U} = [U_1|U_2]$ is an 27×2 orthonormal matrix, the columns of which are called the left singular vectors. $\mathbf{V}^{\mathrm{T}}$ is a 2×2 orthonormal matrix, the columns of which are called the right singular vectors. $\mathbf{\Sigma}$ is a 2

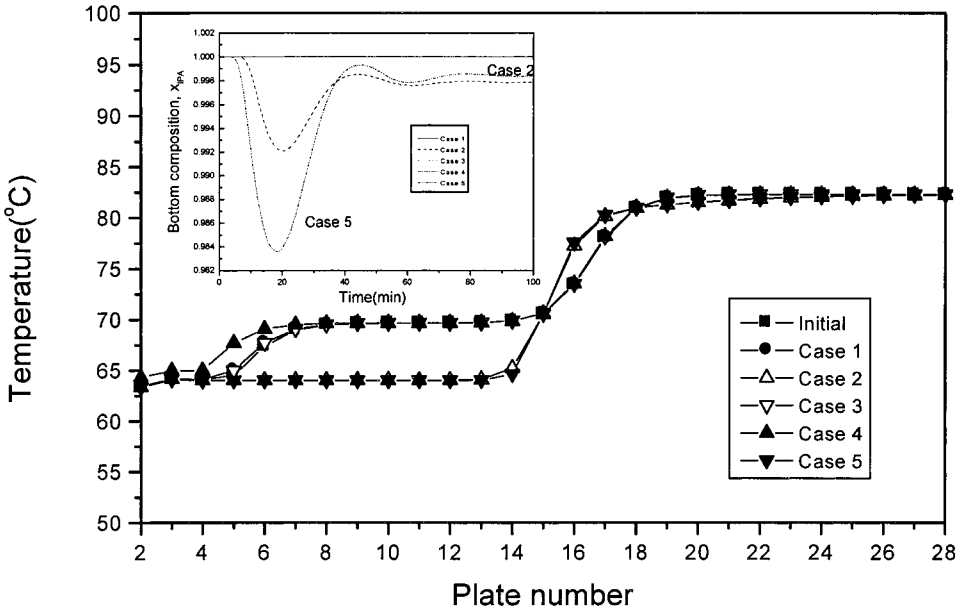

Figure 14. Closed-loop tray temperature profile and composition response for conventional double-loop temperature control scheme.

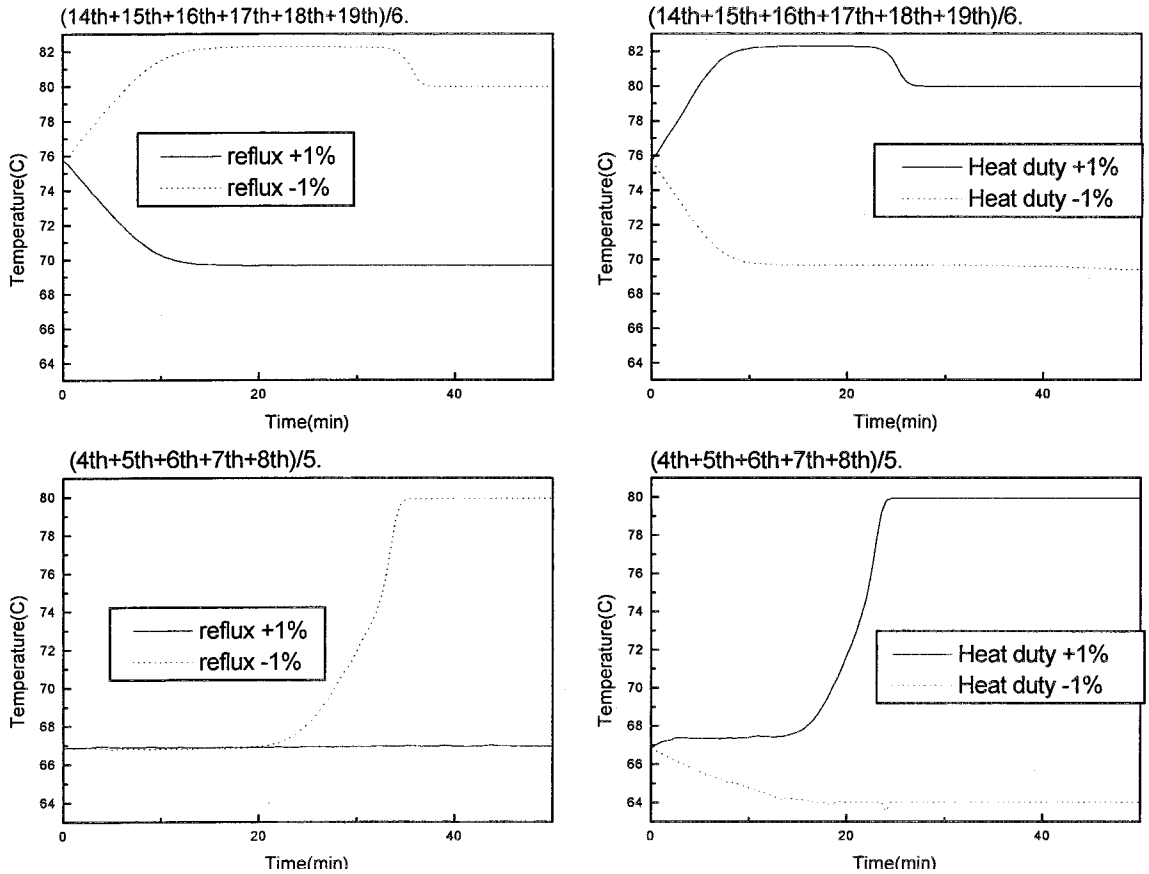

Figure 15. Open-loop step response for the averages of two temperature fronts.

× 2 diagonal matrix of scalars called the singular values and organized in descending order. To trade off between sensor sensitivity and loop interaction, the principal components of U_1 and U_2 vectors are picked as two control points.

In this case study, though, the operating point is at the intersection between a stable and an unstable steady state. Any small perturbation in the manipulated variable will cause the column condition to change drastically, as can be seen previously. Thus, the steady-state gain matrix does not have any useful meaning. On the other hand, when under closed-loop control, the normalized initial rate of change of the sensor variables (the R in Figure 6 and eqs 1 and 2) can be used here instead to do the principal component analysis similar to that above (replacing **K** with R). The result of the modified principal component analysis shows that we should control temperature points at 6th and 17th plates. These are exactly the middle points of the two temperature breaks of profile type II. Because the

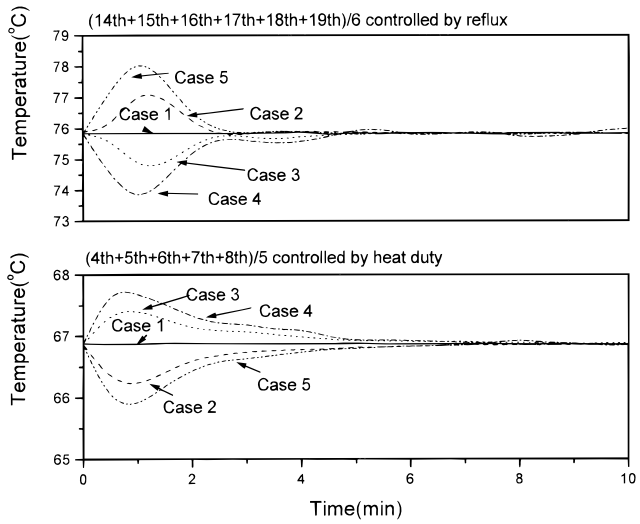

Figure 16. Closed-loop temperature dynamic response for the proposed temperature control scheme.

temperature breaks are rather sharp, average temperatures are used to reduce the strong sensitivity and nonlinearity problems in the control loops.

Figure 15 is the open-loop response of the two controlled variables. From the figure, the effects on the average temperature of the 14th to the 19th plate by reflux and heat duty change are almost the same (but of opposite sign) for the first 10 min. They are also quite linear and symmetric. On the other hand, the effects on the average temperature of the 4th to the 8th plate by reflux and heat duty change are totally different. Increasing the reflux has almost no effect on this variable. Decreasing the reflux has no effect initially but results in a large increase in temperature only after a delay of about 20 min. Increasing and decreasing heat duty both have immediate effects on the average temperature of the 4th to the 8th plate. The open-loop responses show that the average temperature of the break near the column bottom can be controlled by either organic reflux or heat duty. However, the average temperature of the break near the column top can only be controlled by heat duty. The final control loop pairing will have a controlled variable near the top of the column manipulated by heat duty and a controlled variable near the column bottom manipulated by reflux. Therefore, we called this scheme "inverse double-loop average temperature control". The closed-loop responses of the controlled and manipulated variables settle within a few minutes (as shown in Figure 16). Most importantly, all five cases of various feed disturbances can be rejected. The column maintains a type II temperature profile, and the bottom IPA purity is kept at high purity of over 0.9999 for all five cases. Superiority of this scheme over other schemes discussed above is evident.

4. Conclusions

In this work, bifurcation analysis and dynamic simulation were used to investigate the optimum conventional control strategy of an IPA + CyH + H_2O heterogeneous azeotropic column. The process characteristics show that the operating point in the higher reflux region close to critical reflux can obtain a high-purity IPA product with minimum energy consumption and maximum product recovery through the bottom product stream, but this operation is extremely sensitive to feed disturbances. A desired control strategy must be able to prevent column profiles from transforming from type II to other types. The single-loop average temperature control strategy, either two-plate average or multiplate average or supplemented by ratio control using reflux, is not able to maintain the type II profile for disturbances with increased feedwater flow. A conventional double-loop temperature control strategy that uses the temperature at the start and end of the major temperature front performs poorly because strong interaction. To ensure that there is a plateau at 69.3 °C inside the column, two temperature fronts must be established. The average temperature on stages 4−8 is selected as an additional control variable in addition to the average temperatures on stages 14−19. This selection is supported using a modified principal component analysis using initial rates. An open-loop test shows that these variables can only be properly controlled by an inverse double-loop control scheme. The average temperatures on stages 4−8 must be controlled by heat duty while the average temperatures on stages 14−19 are controlled by organic reflux. This control strategy is able to guarantee that the column profile is of type II under various feed changes, keeping the product IPA purity at the desired level while minimizing energy consumption and maximizing product recovery.

Acknowledgment

This work is supported by the National Science Council of the Republic of China under Grant NSC87-2214-E-011-026.

Literature Cited

(1) Widagdo, S.; Seider, W. D. Azeotropic Distillation. *AIChE J.* **1996**, *42*, 96.

(2) Prokopakis, G. J.; Seider, W. D. Feasible Specifications in Azeotropic Distillation. *AIChE J.* **1983**, *29*, 49.

(3) Prokopakis, G. J.; Seider, W. D. Dynamic Simulation of Azeotropic Distillation Towers. *AIChE J.* **1983**, *29*, 1017.

(4) Kovach, J. W., III; Seider, W. D. Heterogeneous Azeotropic Distillation: Experimental and Simulation Results. *AIChE J.* **1987**, *33*, 1300.

(5) Kovach, J. W., III; Seider, W. D. Heterogeneous Azeotropic Distillation: Homotopy-Continuation Methods. *Comput. Chem. Eng.* **1987**, *11*, 593.

(6) Pham, H. N.; Ryan, P. J.; Doherty, M. F. Design and Minimum Reflux for Heterogeneous Azeotropic Distillation Columns. *AIChE J.* **1989**, *35*, 1585.

(7) Ryan, P. J.; Doherty, M. F. Design/optimization of ternary heterogeneous azeotropic distillation sequences. *AIChE J.* **1989**, *35*, 1592.

(8) Widagdo, S.; Seider, W. D.; Sebastian, D. H. Bifurcation Analysis in Heterogeneous Azeotropic Distillation. *AIChE J.* **1989**, *35*, 1457.

(9) Cairns, B. P.; Furzer, I. A. Multicomponent Three-Phase Azeotropic Distillation. 1. Extensive Experimental Data and Simulation Results. *Ind. Eng. Chem. Res.* **1990**, *29*, 1349.

(10) Cairns, B. P.; Furzer, I. A. Multicomponent Three-Phase Azeotropic Distillation. 2. Phase-Stability and Phase-Splitting Algorithms. *Ind. Eng. Chem. Res.* **1990**, *29*, 1364.

(11) Cairns, B. P.; Furzer, I. A. Multicomponent Three-Phase Azeotropic Distillation. 3. Modern Thermodynamic Models and Multiple Solutions. *Ind. Eng. Chem. Res.* **1990**, *29*, 1383.

(12) Pham, H. N.; Doherty, M. F. Design and Synthesis of Azeotropic Distillation: I. Heterogeneous Phase Diagram. *Chem. Eng. Sci.* **1990**, *45*, 1823.

(13) Pham, H. N.; Doherty, M. F. Design and Synthesis of Azeotropic Distillation: II. Residue Curve Maps. *Chem. Eng. Sci.* **1990**, *45*, 1837.

(14) Pham, H. N.; Doherty, M. F. Design and Synthesis of Azeotropic Distillation: III. Column Sequences. *Chem. Eng. Sci.* **1990**, *45*, 1845.

(15) Rovaglio, M.; Doherty, M. F. Dynamics of Heterogeneous Distillation Columns. *AIChE J.* **1990**, *36*, 39.

(16) Wong, D. S. H.; Jang, S. S.; Chang, C. F. Simulation of Dynamics and Phase Pattern Changes for an Azeotropic Distillation Column. *Comput. Chem. Eng.* **1991**, *15*, 325.

(17) Widagdo, S.; Seider, W. D.; Sebastian, D. H. Dynamic Analysis of Heterogeneous Azeotropic Distillation. *AIChE J.* **1992**, *38*, 1229.

(18) Furzer, I. A. Synthesis of Entrainers in Heteroazeotropic Distillation Systems. *Can. J. Chem. Eng.* **1994**, *72*, 358.

(19) Gani, R.; Jørgensen, S. B. Multiplicity in Numerical Solution of Nonlinear Models: Separation Processes. *Comput. Chem. Eng.* **1994**, *18*, S55.

(20) Bekiaris, N.; Meski, G. A.; Morari, M. Multiple Steady States in Heterogeneous Azeotropic Distillation. *Ind. Eng. Chem. Res.* **1996**, *35*, 207.

(21) Müller, D.; Marquardt, W.; Hauschild, T.; Ronge, G.; Steude, H. Experimental Validation of an Equilibrium Stage Model for Three-Phase Distillation. *Inst. Chem. Eng. Symp. Ser.* **1997**, *142*, 149.

(22) Müller, D.; Marquardt, W. Experimental Verification of Multiple Steady States in Heterogeneous Azeotropic Distillation. *Ind. Eng. Chem. Res.* **1997**, *36*, 5410.

(23) Wang, C. J.; Wong, D. S. H.; Chien, I-L.; Shih, R. F.; Liu, W. T.; Tsai, C. S. Critical Reflux, Parametric Sensitivity, and Hysteresis in Azeotropic Distillation of Isopropyl Alcohol + Water + Cyclohexane. *Ind. Eng. Chem. Res.* **1998**, *37*, 2835.

(24) Bozenhardt, H. F. Modern Control Tricks Solve Distillation Problems. *Hydrocarbon Process.* **1988**, June, 47.

(25) Rovaglio, M.; Faravelli, T.; Biardi, G.; Gaffuri, P.; Soccol, S. The Key Role of Entrainer Inventory for Operation and Control of Heterogeneous Azeotropic Distillation Towers. *Comput. Chem. Eng.* **1993**, *17*, 535.

(26) Doedel, E. J.; Wang, X. *AUTO94: Software for Continuation and Bifurcation Problems in Ordinary Differential Equations*; Computer Science Department of Concodia University: Montreal, Canada, 1994.

(27) Schuil, J. A.; Bool, K. K. Three-Phase Flash and Distillation. *Comput. Chem Eng.* **1985**, *9*, 295.

(28) Michelsen, M. L. The Isothermal Flash Problem, Part I: Stability. *Fluid Phase Equilib.* **1982**, *9*, 1.

(29) Dorn, C.; Güttinger, T. E.; Wells, G. J.; Morari, M.; Kienle, A.; Klein, E.; Gilles, E.-D. Stabilization of an Unstable Distillation Column. *Ind. Eng. Chem. Res.* **1998**, *37*, 506.

(30) Chien, I.-L.; Kuo, M. E.; Yu, S. W. A Simple TITO PI Tuning Method Suitable for Industrial Applications. *Symposium on Computer Process Control*, Taipei, Taiwan, Dec 1996; p 24.

(31) Chien, I.-L.; Fruehauf, P. S. Consider IMC Tuning to Improve Controller Performance. *Chem. Eng. Prog.* **1990**, Oct, 33.

(32) Chien, I.-L.; Ogunnaike, B. A. Modeling and Control of A Temperature-Based High-Purity Distillation Column. *Chem. Eng. Commun.* **1997**, *158*, 71.

(33) Moore, C. F. Selection of Controlled and Manipulated Variables. In *Practical Distillation Control*; Luyben, W. L., Ed.; Van Nostrand Reinhold: New York, 1992.

Received for review April 28, 1998
Revised manuscript received November 23, 1998
Accepted November 25, 1998

IE980269F